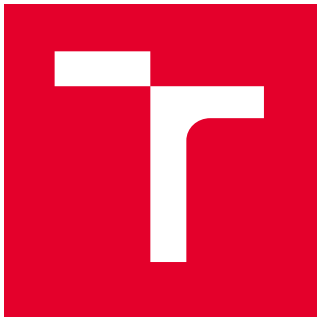

BRNO UNIVERSITY OF TECHNOLOGY

VYSOKÉ UČENÍ TECHNICKÉ V BRNĚ

FACULTY OF MECHANICAL ENGINEERING

FAKULTA STROJNÍHO INŽENÝRSTVÍ

INSTITUTE OF SOLID MECHANICS, MECHATRONICS AND BIOMECHANICS

ÚSTAV MECHANIKY TĚLES, MECHATRONIKY A BIOMECHANIKY

CRITICAL LENGTH PARAMETER USED FOR FATIGUE LIFETIME PREDICTIONS OF NOTCHED SPECIMENS

VYUŽITÍ KRITICKÉHO DÉLKOVÉHO PARAMETRU PRO PREDIKCE ÚNAVOVÉ ŽIVOTNOSTI VRUBOVANÝCH TĚLES

SHORTENED VERSION OF DISSERTATION THESIS

ZKRÁCENÁ VERZE DISERTAČNÍ PRÁCE

AUTHOR — **Ing. Kamila Kozáková**

AUTOR PRÁCE

SUPERVISOR — **doc. Ing. Jan Klusák, Ph.D.**

ŠKOLITEL

BRNO 2025

ABSTRACT

Fatigue life is a key aspect in the design of geometries of notched components subjected to cyclic loading. However, accurate prediction remains a challenge and various approaches are still being developed. One such approach is the theory of critical distances (TCD), which was used in this dissertation. The aim of the work was to develop a fatigue life prediction method for notched metallic specimens based on TCD, experimentally validate its applicability for fatigue life prediction, and propose a modification of the method to achieve more accurate results. Fatigue tests were carried out on smooth and notched specimens made from different materials using an ultrasonic pulsator. On the basis of the experimental data and numerical analyses, the values of the critical distance were determined. This critical distance, including the proposed modification, was then used to predict the fatigue life of notched specimens in both the high-cycle and gigacycle fatigue domains. The predictions were compared with the experimental data. It was found that the critical distance decreases with increasing number of cycles. It also depends significantly on the notch radius, and therefore the critical length parameter must always be adjusted before making predictions. The study extends the application of the TCD to the high-cycle and giga-cycle fatigue domains, provides an analysis of the critical parameter for various notch geometries, and proposes a modification of the theory leading to more accurate predictions.

KEYWORDS

material fatigue, notches, theory of critical distances, critical distance, fatigue life predictions

ABSTRAKT

Únavová životnost je klíčovým aspektem při návrhu geometrie cyklicky namáhaných vrubovaných součástí. Přesná predikce je však stále výzvou a tyto přístupy se dodnes vyvíjí. Jedním z těchto přístupů je teorie kritických vzdáleností, která byla v dizertační práci využita. Cílem práce bylo navrhnout predikční metodu pro únavovou životnost kovových vzorků s vrubem založenou na teorii kritických vzdáleností, experimentálně ověřit vhodnost této metody pro predikci únavové životnosti a navrhnout její modifikaci směřující k přesnějším výsledkům. Byly provedeny únavové zkoušky hladkých a vrubovaných vzorků různých materiálů za použití ultrazvukového pulsátoru. Na základě těchto experimentálních dat a numerických analýz byly určeny hodnoty kritické vzdálenosti. Tato kritická vzdálenost, včetně její navržené modifikace, byla využita k predikci únavové životnosti vrubovaných vzorků v oblasti vysokocyklové a gigacyklové únavy, přičemž výsledky byly srovnány s experimentálními daty. Bylo zjištěno, že se kritická vzdálenost s rostoucím počtem cyklů zmenšuje. Významně také závisí na velikosti poloměru vrubu, proto je nutné délkový parametr před predikcí vždy modifikovat. Práce rozšiřuje aplikaci teorie kritických vzdáleností do oblasti vysokocyklové a gigacyklové únavy, přináší analýzu kritického parametru různých vrubů a navrhuje modifikaci teorie kritických vzdáleností vedoucí k přesnějším predikcím.

KLÍČOVÁ SLOVA

únava materiálu, vruby, teorie kritických vzdáleností, kritická vzdálenost, predikce únavové životnosti

Contents

Introduction

When designing cyclically loaded components, it is necessary to properly select several factors that affect material fatigue. One of the assessed aspects is the choice of material, where it is necessary to consider the operating environment in which the component operates and the required mechanical properties. Another factor that significantly affects the service life of the components is the geometry of the component. The presence of notches, holes, welds, and surface defects leads to a reduction of the service life. Other factors that affect material fatigue include surface treatment, corrosion, size of components, frequency of loading, and testing temperature. However, these factors are not the subjects of this study. The research is focused on the effect of notches on the service life of components and the fatigue lifetime predictions of specimens (and components) with notches.

Fatigue life estimation of notched components can be made using the correction factors, the most well-known method is the Endurance Limit Modifying Factors. This method is based on the adjustment of the fatigue limit of a reference sample, considering the influence of size, surface quality, notch size, etc. The detailed description of the method can be found in Shigley's Mechanical Engineering Design [1]. This method was designed for specific materials; therefore, it has limited applicability and could lead to over-design and unnecessary costs. Another method of evaluating notched components is the local stress-strain approach. This approach is effective for low-cycle fatigue assessments, where plastic deformation in large scale is present. In the high-cycle fatigue or very high-cycle fatigue region, the material behavior is macroscopically elastic, and the accuracy of the approach decreases. For a longer fatigue life, methods such as the theory of critical distances may be more effective.

The Theory of Critical Distances (TCD) is the name given to a group of theories used to predict the effects of stress concentrators and short cracks. The TCD is an extension of linear elastic fracture mechanics (LEFM). These methods use results from finite element analysis (FEA) or other computer-based methods to determine stress states. There are several variations of TCD, the first TCD methods were discovered 70 years ago, although their heyday came with the availability of the finite element method. In the last decades, TCD methods have been intensively developed and applied in various fields of research, but there are still unanswered questions. The aim of this thesis is to formulate a methodology to determine the length parameter for different selected materials, to verify the applicability of the TCD in the field of the high-cycle and gigacycle fatigue region and to propose modifications leading to more accurate predictions.

1 State of the art

Fatigue life is an important characteristic of engineering component and can be sub-divided into:

- Low Cycle Fatigue (LCF) - up to 10^5 cycles to failure,
- High Cycle Fatigue (HCF) - between 10^5 and 10^8 cycles to failure,
- Very-high Cycle Fatigue (VHCF) - over 10^8 cycles to failure.

1.1 Very-high cycle fatigue

In the past, people assumed that if a component could withstand 10^7 cycles without failure, the material is loaded below its fatigue limit, below which an infinite number of loading cycles can be applied. With progress in technology, the required fatigue life exceeds 10^8 cycles, and at the same time it was shown that some materials do not exhibit the fatigue limit, but their S-N curve decreases even beyond 10^7 or 10^8 cycles [2].

Non-ferrous alloys like aluminium alloys have a decreasing stress-life response and their fatigue life reaches 10^8-10^{10} load cycles. There is no well-defined stress below which these alloys do not fail, therefore, fatigue is characterised by fatigue strength at N_f cycles. On the other hand, some ferrous materials exhibit a fatigue limit [3].

When we take a conventional device that operates at a frequency of 25 Hz, it runs for 46 days to reach 10^8 cycles while testing a sample. Testing such long fatigue lives using conventional fatigue testing machines is very time-consuming and expensive, and for that reason piezoelectric testing machines are used. The ultrasonic piezoelectric transducer can reach 10^{10} cycles in less than one week. However, testing with these high frequencies is linked with the disadvantage of increasing the temperature of the specimen during the fatigue test, and hence cooling is required (water or air cooling). The comparison of the time demand of conventional fatigue tests and ultrasonic fatigue tests is shown in Table 1.1.

	10^7 cycles	10^8 cyles	10^9 cycles
Conventional fatigue tests (25 Hz)	$\approx$ 4.6 days	$\approx$ 46 days	$\approx$ 15.4 months
Ultrasonic fatigue tests (20 kHz)	$\approx$ 8.3 min	$\approx$ 83 min	$\approx$ 14 hours

Table 1.1: Comparison of testing times using conventional and ultrasonic fatigue testing machine [4]

The first ultrasonic fatigue machine was developed in 1950 by Warren P. Mason in the United States. This prototype of ultrasonic fatigue testing machine is used

as a basis for contemporary fatigue testing equipment. With the development of computer sciences, several laboratories have developed their own machines: S. Stanzl in Austria, C. Bathias in France, H. Ishii in Japan and A. Puškár in Slovakia. There are several designs of ultrasonic machines, but all of them consist of three main components: an ultrasonic generator, a piezoeletric transducer/converter, an ultrasonic horn/sonotrode, see Fig. 1.1 [5, 6].

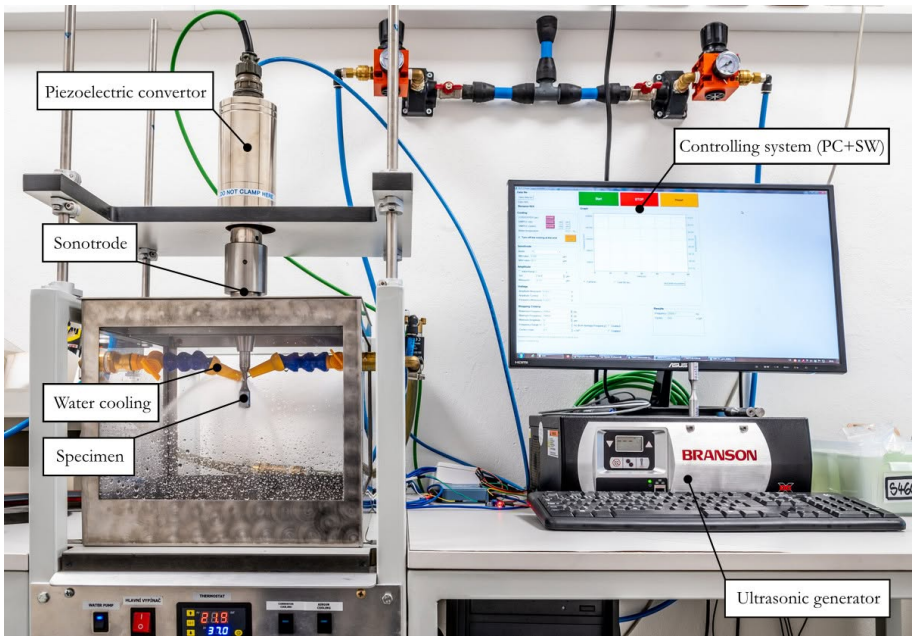

Fig. 1.1: Gigacycle fatigue testing configuration at IPM, CAS

The test specimens are designed on the basis of the wavelength of the operating frequency. Even higher frequencies for fatigue testing can be reached; however, 20 kHz has become the norm for ultrasonic fatigue testing machines, mainly due to power supplies, transducers, and various safety considerations [7, 8].

Ultrasonic fatigue tests have shown that a fracture can occur at 10^9 or more cycles. Bathias compared fatigue crack initiation in LCF, HCF, and VHCF ranges using specimens with perfectly polished surfaces. At high loading amplitudes (LCF), there are usually many crack initiation sites on the surface, originating from dislocation slip. At lower amplitudes (HCF), there are similar crack initiation sites at the surface but less than under LCF conditions. At still lower loading amplitudes (VHCF), there are almost no crack initiation sites at the surface and almost no crack growth from the surface into the interior. In the VHCF region, cracks can be formed at internal material defects (inclusions, microstructure inhomogenities or pores) and can grow, so called "fish-eye" is formed. These cracks slowly outwards and can be life-determining [9, 10, 11].

1.2 Notch characterisation

Geometrical discontinuities are unavoidable in design. Holes, fillets, shoulders, and grooves, generally termed notches, commonly exist in engineering components. When these components are subjected to external loads, geometrical changes act as stress raisers. Notches require special attention, as their presence reduces the resistance of a component to fatigue failure. At such locations, locally higher stresses can cause fatigue crack initiations and consequently their growth [12, 13].

The elastic stress concentration factor K_t may be employed to provide a quantitative description for stress concentration severity of notch, where

$$K_\mathrm{t} = \frac{\sigma_\mathrm{max}}{\sigma_\mathrm{nom}} \tag{1.1}$$

is the ratio of the maximum stress at a notch tip and the nominal stress under pure elastic state [12]. The stress-concentration factor K_t is dependent on the geometry of the notched component and on the geometry of the loading forces (type of loading, e.g. tension, bending, torsion) [14]. However, K_t cannot effectively characterize the relationship between fatigue strengths of smooth and notched specimens, because it generally yields conservative predictions on the endurance of engineering components under cyclic loading [12].

Due to this fact, the fatigue notch factor (fatigue strength reduction factor) K_f is introduced. The fatigue notch factor K_f describes the influence of the notch effect on fatigue strength of interest and is defined by:

$$K_\mathrm{f} = \frac{S_\mathrm{e}}{S_\mathrm{n}}, \tag{1.2}$$

where S_e is fatigue strength of smooth and S_n is fatigue strength of notched specimen [12]. If the notch has a small radius r at its tip, K_f is smaller than K_t. However, for a large radius r, K_f may be essentially equal to K_t. Generally, K_f is calculated from empirical equations, which are based on statistics, reversed yielding, or crack growth.

Commonly used methods for fatigue evaluation of metallic notched components are: nominal stress approach [15], local stress strain approach [16, 17], weighting control parameters-based approaches [18], and critical distance theories [19, 20, 21, 12]. The last one is the base for the method used in the presented work.

Theory of Critical Distances (TCD) is an efficient strategy for notch effect analyses. TCD assumes that the highly-stressed zone can be quantified on the basis of effective stress, σ_eff. According to the different critical distance definitions, four types of TCD methods can be summarized, see Fig. 1.2.

The Point Method (PM) is the simplest of the methods. PM defines effective stress at a single point ahead of the notch root. The Line Method (LM) defines

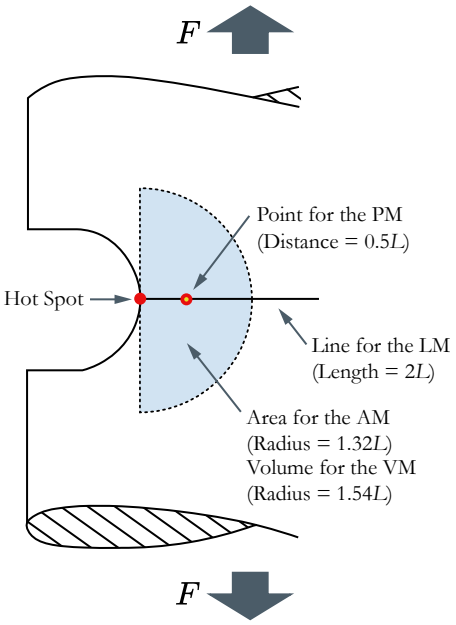

Fig. 1.2: Different forms of TCD: Point Method (PM), Line Method (LM), Area Method (AM), Volume Method (VM) [12]

effective stress as the average stress over a certain distance starting at the notch root. In addition to PM and LM, there are the Area Method (AM) and the Volume Method (VM). These methods define effective stress as the average stress in the area in the vicinity of the notch and in the hemispherical volume, respectively [12].

An important issue in the application of TCD in notch fatigue analyses is the calculation of the critical distance. The value of the critical distance for fatigue predictions can be obtained from a formula or determined from experimental data. The commonly used length parameter for fatigue limit predictions is given by [12, 22]:

$$L = \frac{1}{\pi}\left(\frac{\Delta K_{\mathrm{th}}}{\Delta\sigma_0}\right)^2, \tag{1.3}$$

where ΔK_{th} represents the range of the threshold stress intensity factor, and $\Delta\sigma_0$ represents the fatigue limit range of plain specimen (both determined under the same load ratio, R). The Line method, which was used in this research, can be expressed as follows:

$$\text{LM} \qquad \sigma_{\mathrm{eff}} = \frac{1}{2L}\int_0^{2L}\sigma(r)\mathrm{d}r, \tag{1.4}$$

A component containing a stress concentrator is assumed to be at its fatigue limit conditions when a defined effective stress equals the material plain fatigue limit:

$$\Delta\sigma_{\mathrm{eff}} = \Delta\sigma_0 \tag{1.5}$$

2 Dissertation aims and objectives

The TCD approaches usually use a constant value of the critical distance obtained from formula. However, the constant distance does not provide a reliable prediction of the fatigue life of the notched specimens. The critical distance varies for different fatigue regions. In addition, experimental studies of the TCD methods, especially in the area of high-cycle and very-high-cycle fatigue, are very limited and the applicability of this method in these fatigue regions is not properly known. All TCD methods contain an implicit material or model parameter that is not explicitly specified. It is always necessary to calibrate the method to obtain accurate results. In this work, our aim is to identify these parameters in such a way as to enable the most accurate possible lifetime predictions based on known input data.

The aim of the thesis is to propose a method based on TCD approach and to apply it to experimental fatigue data of various materials and various notch radii and to assess the applicability of the method in the HCF and VHCF regions. The aim of the thesis is to find the dependency of the critical length parameter on the number of cycles and the radius of the notch, analyse the critical values, and calculate fatigue lifetime predictions of various notches using the model notch. Based on the comparison of the predicted fatigue data and the experimental results, adjustments to the methodology can be proposed.

To reach the project goal, the solution of the problem will be divided into two parts: experimental and theoretical, in which the following tasks were set:

Experimental part:

- design of specimens using FEA (modal analysis),
- determination of axial stress distribution and stress factors using FEA (harmonic analysis),
- measurement of the dynamic modulus of studied materials,
- description of the microstructure of studied materials,
- ultrasonic fatigue tests of smooth and notched specimens,
- analysis of the fracture surfaces.

Theoretical part:

- mathematical formulation of the method based on the TCD,
- applying the method to the S-N data and calculating the length parameter,
- predictions of fatigue lifetime of notched specimens based on the length parameter,
- analysis of results,
- modifications of the prediction method.

3 Methodology

To verify the applicability of the TCD in the HCF and VHCF regimes, the following methodology was applied:

- Design and manufacturing of smooth and notched specimens (six types of notched specimens) for six different materials,
- Fatigue testing using an ultrasonic pulsator operating at 20 kHz,
- Numerical modeling of stress field under cyclic loading using ANSYS software,
- Calculation of the critical distance based on experimental fatigue data and axial stress distribution in the vicinity of the notches,
- Fatigue lifetime predictions of notched specimens using the calculated critical distance,
- Comparison of predicted fatigue lifetimes with experimental results,
- Evaluation and possible refinement of the TCD approach based on observed discrepancies.

3.1 Numerical analysis and fatigue testing

Finite Element Method software is used to design the geometry of the specimens and to determine the stress distribution in them. The geometries of the smooth and notched specimens are created using the ANSYS APDL scripting language. Input parameters such as dynamic Young's modulus and Poisson's ratio are determined using the impulse excitation technique at IMCE HT1600 and together with the mass density are then used in numerical modeling. Conducting fatigue tests in the gigacycle regime is possible using an ultrasonic fatigue testing machine, which typically works at a frequency of 20 kHz. For that reason, samples are designed to have a longitudinal modal shape at a resonant frequency of 20 kHz. To achieve the intrinsic frequency of longitudinal vibrations of the sample, close to 20 kHz, the length of the sample is found during the modal analyses. Smooth and notched samples with notch radii of 0.1 mm, 0.2 mm, 0.4 mm, 0.8 mm, 1.5 mm and 3.0 mm are designed and machined from each experimental material. Because different sizes of notches are used, the length of these samples also varies. The presence of a notch affects the natural frequencies of the sample. All specimens have the same narrowest diameter of 5 mm, and the diameter of the heads of the specimens is 14 mm. The depth of the notch is 0.5 mm in all cases. The drawing of the notches is shown in Fig. 3.1.

Knowledge of the axial stress distribution of smooth and notched specimens is required for further analysis and calculation of the critical length parameter. During a harmonic analysis, the end of the sample is loaded with a displacement amplitude

of $u = 1$ µm. The distribution of axial stress σ_y is calculated as a function of the distance x from the tip of the notch to the center of the sample; see Fig. 3.2.

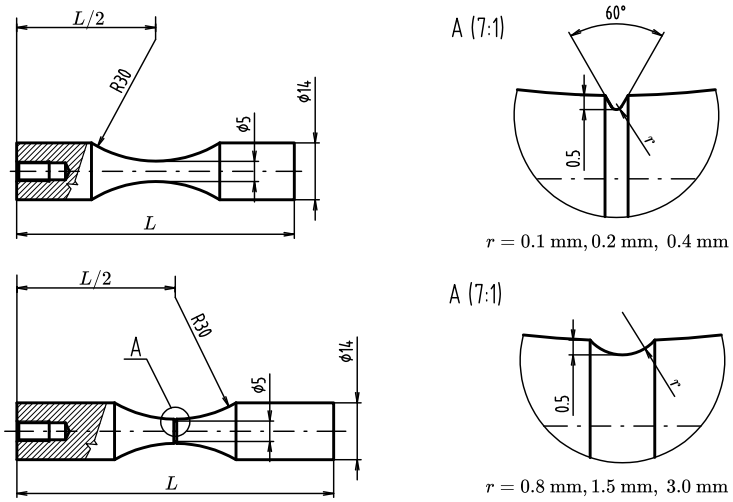

Fig. 3.1: Design of smooth and notched specimens with notch radius r

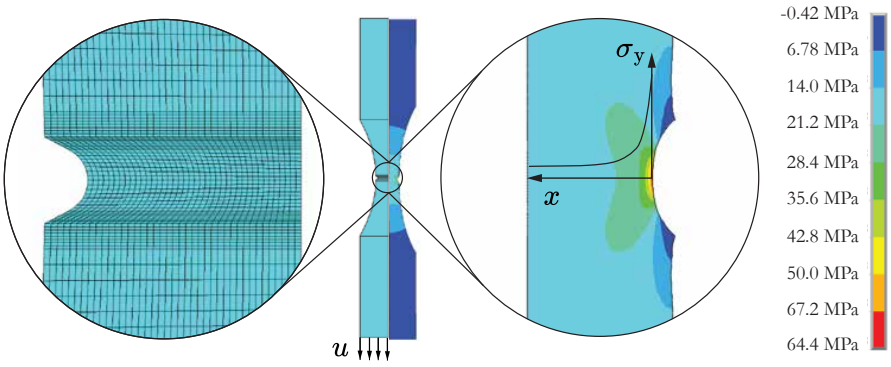

Fig. 3.2: FEA: mesh refinement around a notch with radius $r = 0.4$ mm, axial stress distribution from harmonic analysis, $u = 1$ μm, stainless steel

Fatigue tests are performed using an ultrasonic fatigue loading system built at the Institute of Physics of Materials of the Czech Academy of Sciences (IPM, CAS), see Fig. 1.1. The fatigue tests are performed under uniaxial and symmetric tension-compression loading, $R = -1$, at room temperature. To avoid increasing the temperature of the specimens, the central part of the specimen must be cooled by water or air.

3.2 Determination of the critical distance

The critical distance is determined from S-N (stress amplitude - number of cycles to failure) curves measured on smooth specimens and specimens with a model notch. To analyse the dependence of the critical distance on the radius of the notch, the critical distance is calculated from the six pairs of smooth and notched curves (r = 0.1, 0.2, 0.4, 0.8, 1.5 and 3.0 mm) of each material. The critical distance calculated from the model notch ($r = 0.8$ mm) is used for fatigue lifetime predictions.

Looking at the fitted fatigue data of smooth and notched specimens, the notched specimens usually have a shorter fatigue life. For a given number of cycles to failure, N_f, the corresponding nominal stress amplitudes for notched specimens ($\sigma_\mathrm{a}^\mathrm{n}$) and smooth ($\sigma_\mathrm{a}^\mathrm{s}$) specimens can be read, as shown in Fig. 3.3 (left). The applied nominal stress amplitude $\sigma_\mathrm{a}^\mathrm{n}$ corresponds to the average stress value over the entire cross section of the notched specimen; see Eq. 3.1, and middle scheme in Fig. 3.3.

$$\sigma_\mathrm{a}^\mathrm{n} = \frac{1}{D}\int_0^D \sigma_y^\mathrm{n}\mathrm{d}x \tag{3.1}$$

Then, in the same axial stress distribution of notched specimen, we can find the distance l_cr, for which the average stress over this distance is equal to the nominal amplitude of the applied stress of the smooth specimen taken from the S-N curve; see Eq. 3.2, and Fig. 3.3, right. The average stress over the critical distance l_cr is given by Eq. 3.3.

$$\bar{\sigma_y^\mathrm{n}}(l_\mathrm{cr}, N_\mathrm{f}) = \sigma_\mathrm{a}^\mathrm{s}(N_\mathrm{f}) \tag{3.2}$$

$$\overline{\sigma_y^\mathrm{n}}(l_\mathrm{cr}, N_\mathrm{f}) = \frac{1}{l_\mathrm{cr}}\int_0^{l_\mathrm{cr}} \sigma_y^\mathrm{n}(N_\mathrm{f})\mathrm{d}x \tag{3.3}$$

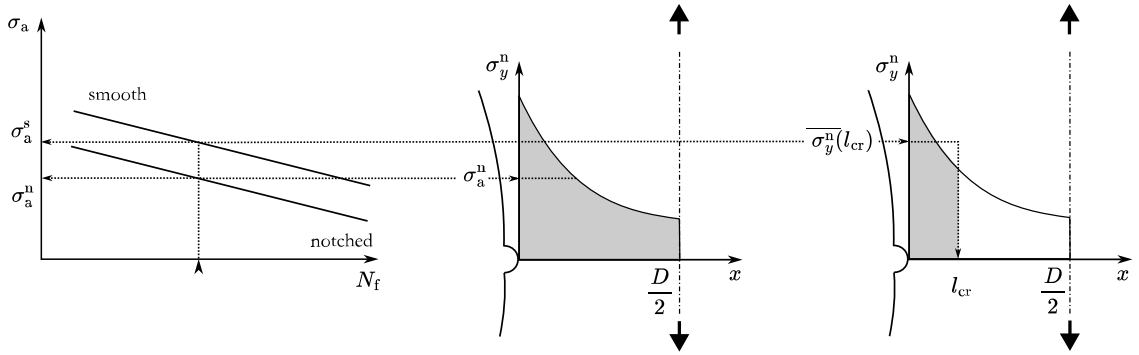

Fig. 3.3: Determination of the critical length parameter at specific number of cycles, N_f

The process of determining the critical distance is repeated through the entire range of numbers of cycles and the dependence of the critical parameter on number of cycles and notch radius is obtained.

3.3 Fatigue lifetime predictions

The dependency of the critical distance of the model notch is used to predict the fatigue life of various notches. It can be said that fatigue lifetime prediction is an inverse procedure to the critical distance determination. For the fatigue life predictions of the notched specimens, the S-N curve of the smooth specimens, the axial stress distribution of the predicted notch, and the critical distance are used. However, the problem is which critical distance shall be used.

In the following predictions, the notch with radius $r = 0.8$ mm is selected as the model notch. For that reason, the critical distance dependence, calculated from S-N curves of smooth and notched samples with a model notch, is denoted as l_{m}, where "m" stays for the model notch. The fatigue lifetimes of other notches are predicted using the critical length parameter l_{p}, where "p" stays for the predicted notch. The accuracy of the fatigue lifetime predictions is assessed by comparing with experimental data. The following three approaches are introduced and compared. The first approach uses the constant critical distance for fatigue predictions; see Eq. 3.4.

$$l_{\mathrm{p}} = l_{\mathrm{m}}(N_{\mathrm{f}} = 10^7 \text{ cycles}) \tag{3.4}$$

In the second approach, it is assumed that the critical distance does not change significantly with different notch radii. Therefore, the critical distance dependence $l_{\mathrm{m}}(N_{\mathrm{f}})$ calculated from a model notch is used directly to predict the fatigue lifetime of notched samples with various notch radii r. The critical distance includes the effect of the number of cycles to failure:

$$l_{\mathrm{p}}(N_{\mathrm{f}}) = l_{\mathrm{m}}(N_{\mathrm{f}}). \tag{3.5}$$

In order to obtain more accurate predictions, the third approach is introduced. In this approach, the critical distance dependence $l_{\mathrm{m}}(N_{\mathrm{f}})$ is modified using stress concentration factors K_{t}. The critical distance dependency for fatigue lifetime predictions of the specific notch radius has the following form:

$$l_{\mathrm{p}}(N_{\mathrm{f}}) = l_{\mathrm{m}}(N_{\mathrm{f}}) \cdot \frac{K_{\mathrm{t,m}}}{K_{\mathrm{t,p}}} \tag{3.6}$$

where $K_{\mathrm{t,m}}$ is the stress concentration factor of the model notch and $K_{\mathrm{t,p}}$ is the stress concentration factor of the predicted notch. In contrast to the previous approaches,

the critical distance used for predictions depends on the notch radius of the predicted notch.

To predict the fatigue life of the notched specimens, the axial stress distribution in the vicinity of the notch is essential. To reduce the number of calculations, the axial stress normalized by the nominal applied stress is used (the average stress over the entire cross section is equal to 1), see Eq. 3.7, where $\sigma_{\mathrm{y}}^{\mathrm{n}}$ represents the axial stress distribution of the notched specimen (predicted) loaded with the nominal stress and $\sigma_{\mathrm{a}}^{\mathrm{n}}$ represents the nominal applied stress.

$$\sigma_y^{\mathrm{n}*} = \frac{\sigma_{\mathrm{y}}^{\mathrm{n}}}{\sigma_{\mathrm{a}}^{\mathrm{n}}}\ [-], \tag{3.7}$$

To predict the fatigue life of notched specimens, the fatigue life of smooth specimens, the critical distance, and the axial stress distribution of the predicted notch must be known. The predicted nominal stress amplitude of notched specimens $\sigma_{\mathrm{a}}^{\mathrm{n}}(N_{\mathrm{f}})$ is given by Eq. 3.8, where $\sigma_{\mathrm{a}}^{\mathrm{s}}(N_{\mathrm{f}})$ is the nominal stress amplitude of smooth specimens read from the S-N curve for a particular number of cycles to failure, $\overline{\sigma_y^{\mathrm{n}*}}(l_p)$ is the average normalized axial stress of the predicted notch calculated over the prediction distance l_{p}. The critical distance for predictions can be constant, dependent on the number of cycles, or notch radius r dependent, Eq. 3.4, 3.5, 3.6.

$$\sigma_{\mathrm{a}}^{\mathrm{n}}(N_{\mathrm{f}}) = \frac{\sigma_{\mathrm{a}}^{\mathrm{s}}(N_{\mathrm{f}})}{\overline{\sigma_y^{\mathrm{n}*}}(l_{\mathrm{p}})} \tag{3.8}$$

The prediction procedure is shown in Fig. 3.4. The scheme describes the determination of a single point of S-N curve of predicted notched specimens, the process is repeated for all numbers of cycles. First, $\sigma_{\mathrm{a}}^{\mathrm{s}}(N_{\mathrm{f}})$ is read from the experimental fatigue curve, similarly, the critical distance for the predictions is known, and this critical distance l_{p} is applied to the normalized axial stress distribution of the predicted notch, the average normalized axial stress over the critical distance l_{p} is calculated. The predicted nominal stress amplitude is determined using Eq. 3.8.

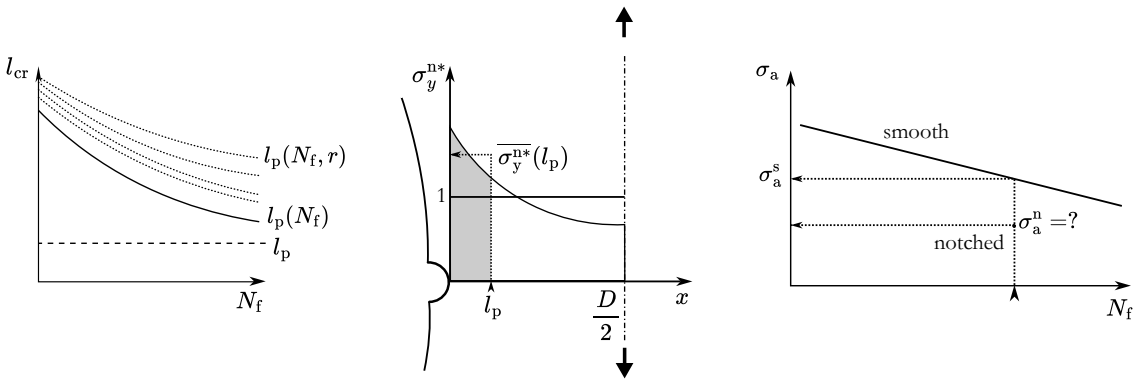

Fig. 3.4: Determination of the predicted stress amplitude of the notched specimen

4 Results

Notched and smooth samples made of aluminum alloy AW7075, 304L stainless steels (two modifications 1.4306 and 1.4307) and steels S960QL, S690QL, and S460NL were tested. Before fatigue tests are performed, the microstructure of experimental materials was studied, surface quality was checked and numerical analysis of all smooth and notched specimens was performed. Fatigue specimens were machined in the workshop of IPM, CAS. All central sections of the smooth specimens were polished with SiC paper up to P4000, and, if necessary, further polished with diamond paste. Notched specimens were left as machined. Only smooth and notched stainless steel specimens were additionally electropolished.

4.1 Pretest preparations

The stress distribution around the notch, determined by numerical modeling, is a necessary part of determining the critical distance. The input parameters for the numerical analyses were measured using the impulse excitation technique and are listed in Tab. 4.1. In addition to the elastic constants, the density of the material was also determined and is included in the same table.

Table 4.1: Input parameters for numerical modeling

Material	E_{d} [GPa]	ρ [kg/m^3]	μ [-]
AW7075	72.15	2807.95	0.33
1.4306	199	7890	0.3
1.4307	199	7890	0.3
S960QL	211.54	7820	0.3
S690QL	220.9	7815	0.3
S460NL	211.45	7800	0.3

Fig. 4.1 shows the distribution of axial stress of all notched and smooth specimens normalized by the nominal applied stress amplitude σ_{a}:

$$\sigma_y^* = \frac{\sigma_y}{\sigma_{\mathrm{a}}} \tag{4.1}$$

From these axial stress distributions it is possible to determine the elastic stress concentration factors K_{t} of studied notched specimens according to Eq. 1.1. When the stress is normalized, the elastic stress concentration factors are equal to their maximum stress; see the Tab. 4.2. The maximum stresses increase significantly as the radius decreases in size.

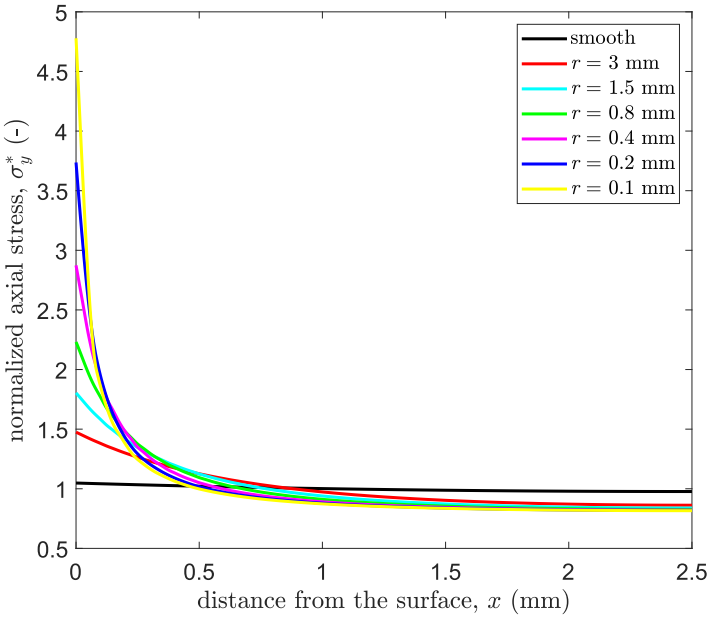

Fig. 4.1: Normalized axial stress distributions of notched specimens

Table 4.2: The elastic stress concentration factors K_t (-)

notch radius r (mm)	3	1.5	0.8	0.4	0.2	0.1
K_t (-)	1.47	1.80	2.23	2.87	3.74	4.78

4.2 Fatigue data

The output of fatigue tests are dependencies of number of cycles to fracture, N_f, on stress amplitude, σ_a. Six different radii on notched specimens and smooth specimens made of six materials were tested. Fatigue data of broken specimens are approximated by exponential equation (Basquin's function).

$$\sigma_\mathrm{a} = A \cdot N_\mathrm{f}^B \tag{4.2}$$

Empty points represent runouts, i.e. specimens that have not broken after reaching 1×10^{10} cycles. As can be seen in the following figures, the notches have a negative effect on fatigue life. Fatigue data of notches with sharper radii are shifted to the lower lifetimes taking into account the same stress amplitude. This behaviour is broken only in one material, namely aluminium alloy.

The fatigue data of smooth and notched specimens made of aluminium alloy AW7075 are shown in Fig. 4.2. The fatigue data of aluminium alloy specimens range between 50 and 200 MPa. Comparison of the curves shows that the slope of the curve for $r = 1.5$ mm differs significantly from others. Another strange feature is

the interchange of curves describing notched specimens with radius $r = 0.8$ mm and $r = 0.4$ mm. This anomaly can be explained by the influence of machining process, when the surfaces of notches with notch radii $r = 0.8,\ 1.5,\ 3$ mm are not perfectly smooth and contain micro notches compared to notch radii $r = 0.1,\ 0.2,\ 0.4$ mm. All broken specimens range between 10^5 and 10^{10} cycles.

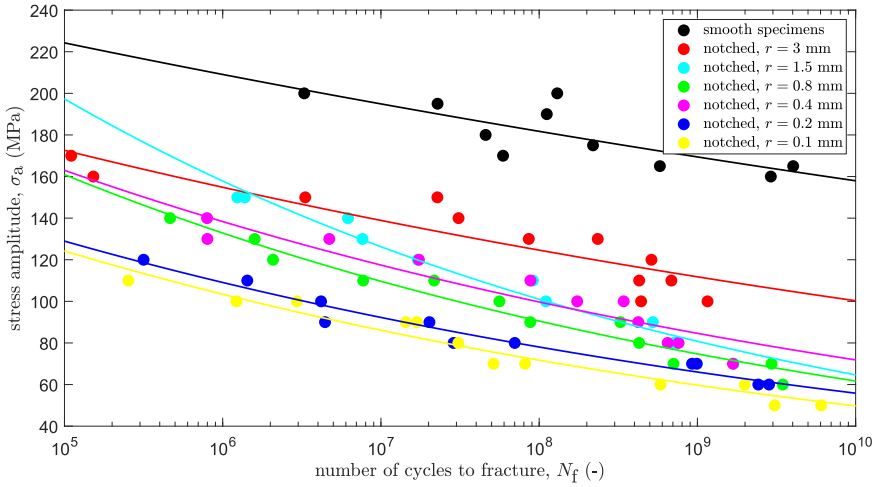

Fig. 4.2: AW 7075 aluminum alloy: fatigue data

Fig. 4.3 shows fatigue data of 1.4306 stainless steel specimens. The fatigue data range between 100 and 250 MPa. There are no broken specimens behind 10^8 cycles. An approximation curve of specimens with notch radius $r = 0.2$ mm is located slightly under the approximation curve of notched specimens with notch radius $r = 0.1$ mm, although this difference is not significant and can be caused by experimental scatter of fatigue data.

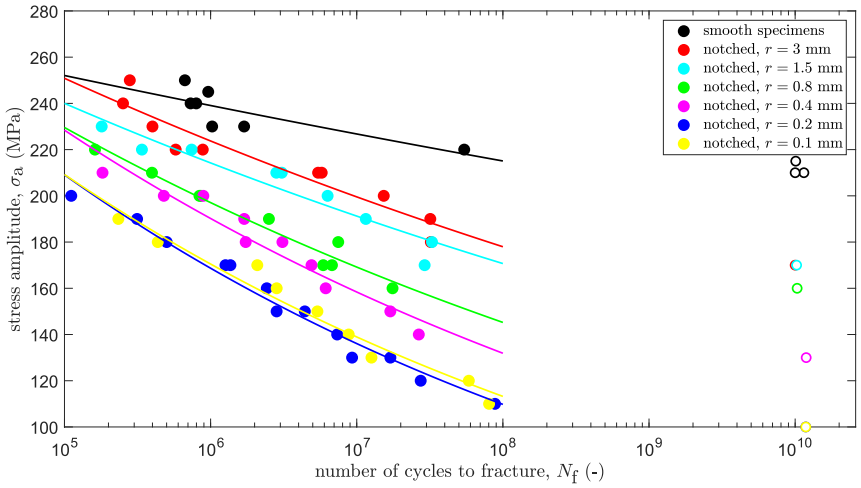

Fig. 4.3: 1.4306 stainless steel: fatigue data

Another tested material is S690QL structural steel, see Fig. 4.4. Fatigue life was experimentally determined for stress amplitudes in the range between 130 and 605 MPa. The fitted curves of the smooth and notched specimens are parallel. The fatigue life of broken specimens ranges between 10^5 and 10^7 cycles.

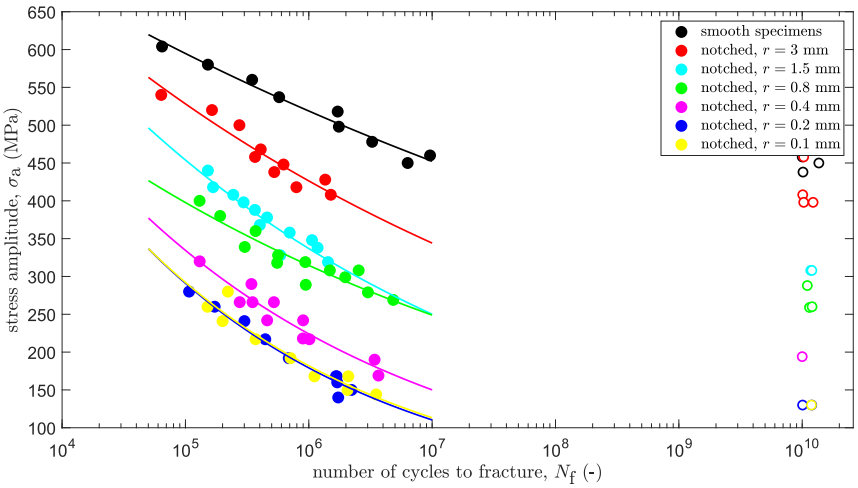

Fig. 4.4: S690QL structural steel: fatigue data

4.3 Critical length parameter

The critical distance is dependent on the notch radius, the number of cycles and material. The critical distance l_{cr} is decreasing with the increasing number of cycles N_f in all cases. The bigger the notch, the bigger the critical distance. This fact can be observed in Fig. 4.5a, 4.5b and 4.5c.

The values of the critical distance are between 0 and 2.5 mm. These limits are given by dimensions of the specimens ($D/2 = 2.5$ mm).

An average critical distance of each material at 10^7 cycles is listed in Tab. 4.3. The greatest values of critical distance are in case of 1.4307 and 1.4306 stainless steels and the smallest value is in case of S960QL structural steel. The relation between the critical distance and yield strength is visible. The critical distance decreases with the increasing value of the yield strength, R_p.

Table 4.3: Comparison of average critical distances at 10^7 cycles (mm)

	1.4307	1.4306	AW7075	S460NL	S690QL	S960QL
$\overline{l_{cr}}(N_f = 10^7)$	0.85	0.73	0.23	0.17	0.10	0.00
R_p (MPa)	266	242	470	491	817	1040

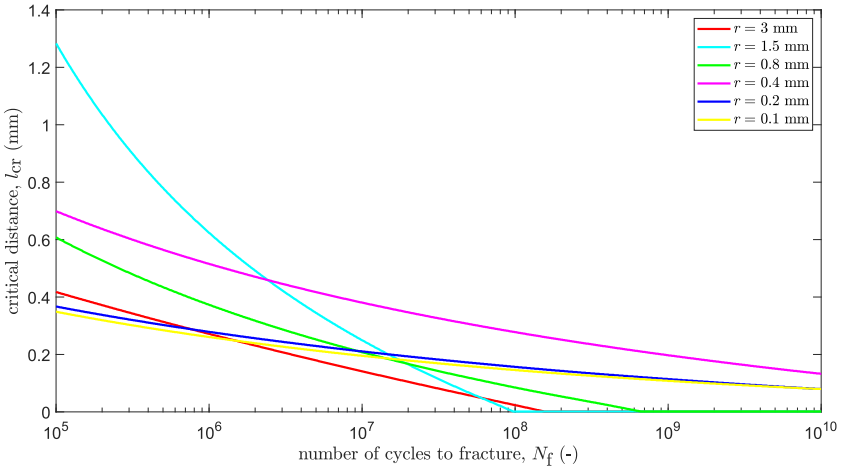

(a) AW7075 aluminum alloy

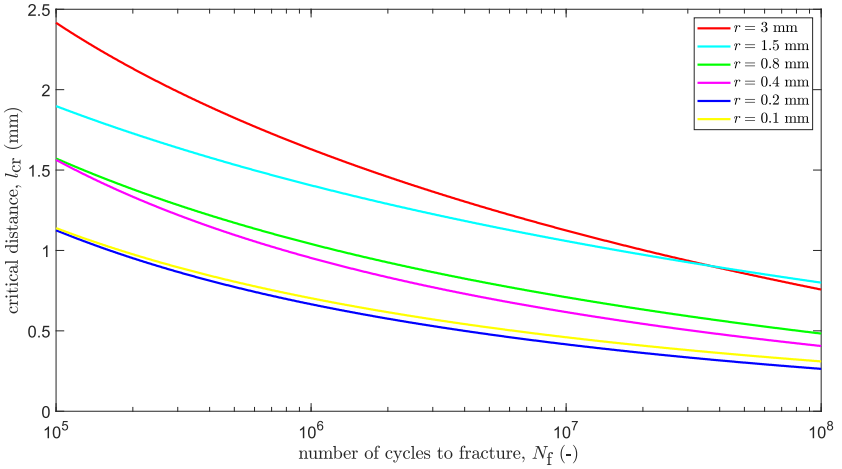

(b) 1.4306 stainless steel

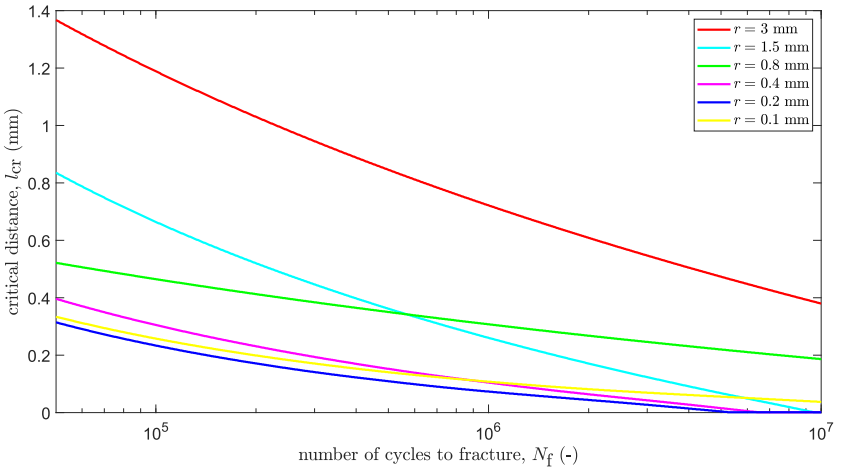

(c) S690QL structural steel

Fig. 4.5: Dependence of critical distance on number of cycles, radius and materials

4.4 Fatigue lifetime predictions

In the following figures, the fatigue predictions are presented. All graphs include the original experimental data (filled points) to assess the success of the predictions (dotted lines). It should be noted that in the following graphs the approximation of broken smooth specimens is not a prediction, this curve is used as an input for fatigue predictions. Three types of predictions are calculated for individual materials and depend on the used critical distance for predictions. The critical parameter of a model notch with radius $r = 0.8$ mm of the respective material was used in the predictions below.

The fatigue lifetime predictions of notched specimens made of AW7075 can be seen in Fig. 4.6. To calculate the predictions using a constant value, a value of 0.2075 mm was used, which represents the size of the critical distance at 10^7 cycles ($r = 0.8$ mm), see Fig. 4.5a. The predictions from constant value of critical distance are safe at lower lifetimes, at higher number of cycles to failure they are non-conservative. The slope of prediction curves is not ideal. Second graph in Fig. 4.6 is calculated from critical distance dependence. The slope of the curves is better than in the previous graph. The fatigue life curves are broken, this break is caused by the zero values of the critical distance after 10^9 cycles. The last graph in Fig. 4.6 represents the fatigue predictions from the modified critical distances. These predictions are close to the experimental data or lead to a safe lifetime estimation.

The fatigue life predictions of 1.4306 stainless steel notched specimens are shown in Fig. 4.7. In the first figure, constant value of critical distance was used, the value of the critical distance at 10^7 cycles ($r = 0.8$ mm) is 0.7091 mm. Using a constant critical distance value does not produce prediction curves with a suitable slope compared to the experimental data. The layout of the curves is also inconsistent with the experimental data. Using the critical distance dependent on number of cycles, the slope of prediction curves is improved, although the predictions of notches smaller than 0.8 mm are unsafe. The third graph in Fig. 4.7 captures the modification using stress concentration factors. The modification leads to safer predictions of sharp notches and a slight upward shift of prediction curves of blunt notches.

The fatigue life predictions of the S690QL stainless steel notched specimens are shown in Fig. 4.8. In the first graph, a constant value of the critical distance 0.1863 mm is used for the predictions. As in the previous cases, using constant values of critical distance yields an inappropriate slope of predicted curves compared to experimental data. Using a critical distance that takes into account the number of cycles improves the slope of the prediction curves. A significant improvement in fatigue life estimations can be observed in the last graph, when the critical distances modified by stress concentration factors were used.

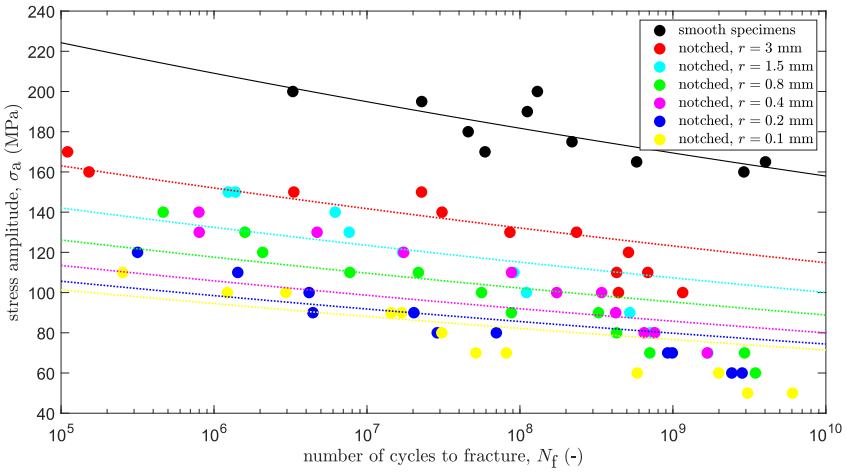

(a) $l_p = l_m(N_f = 10^7 \text{ cycles})$

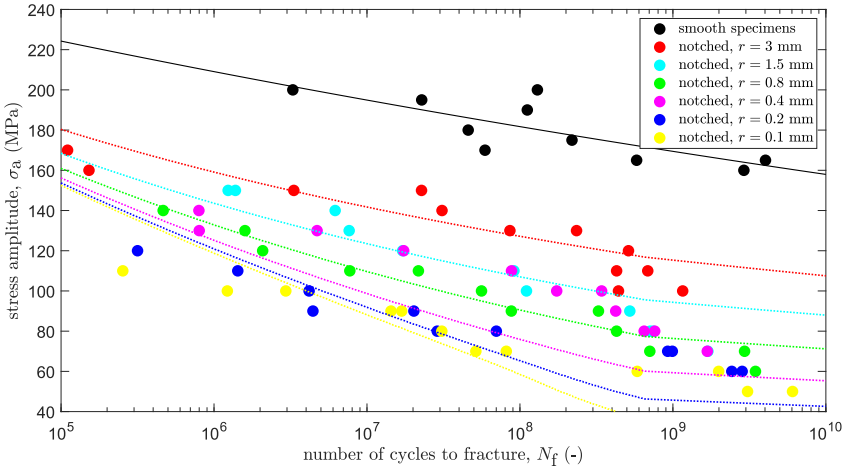

(b) $l_p(N_f) = l_m(N_f)$

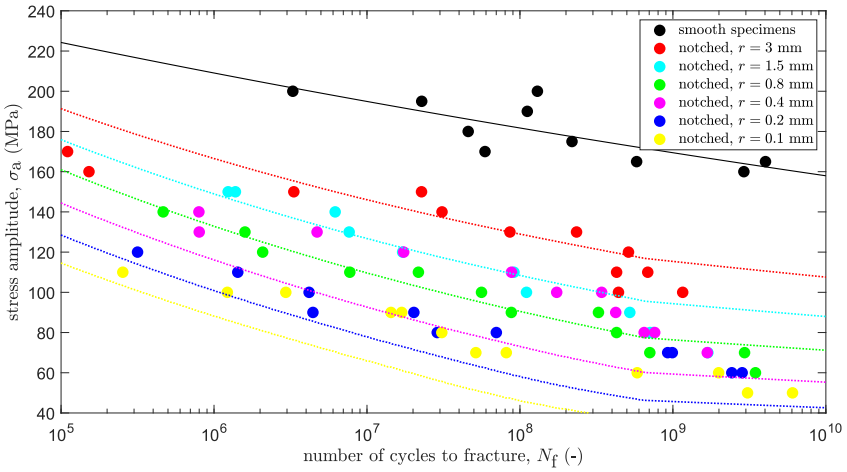

(c) $l_p(N_f) = l_m(N_f) \cdot \frac{K_{t,m}}{K_{t,p}}$

Fig. 4.6: Fatigue lifetime predictions: AW7075, model notch $r = 0.8$ mm

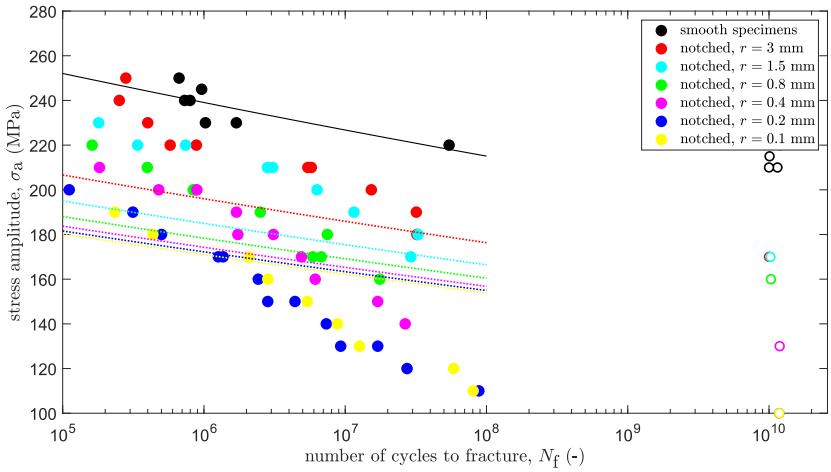

(a) $l_p = l_m(N_f = 10^7 \text{ cycles})$

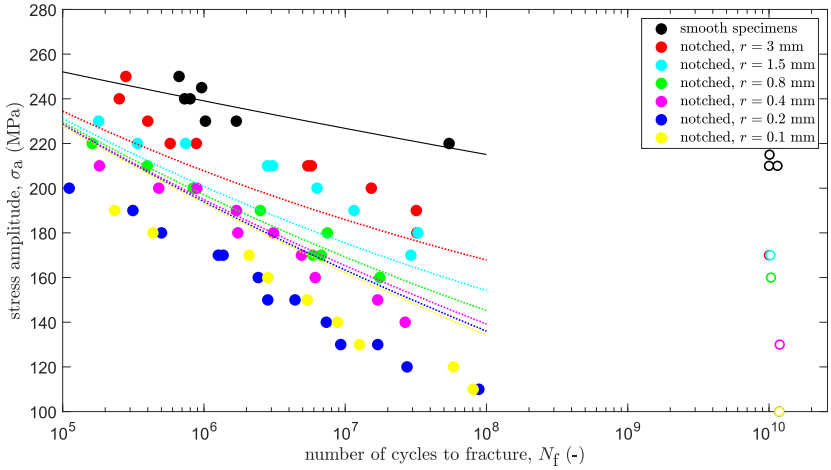

(b) $l_p(N_f) = l_m(N_f)$

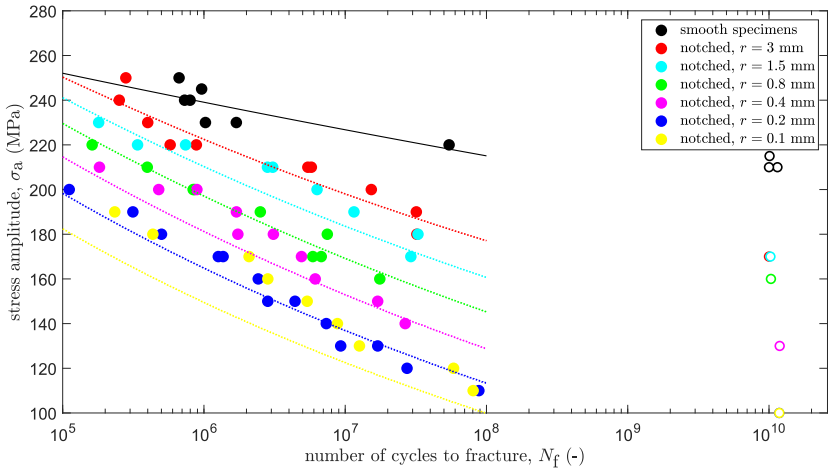

(c) $l_p(N_f) = l_m(N_f) \cdot \frac{K_{t,m}}{K_{t,p}}$

Fig. 4.7: Fatigue lifetime predictions: 1.4306, model notch $r = 0.8$ mm

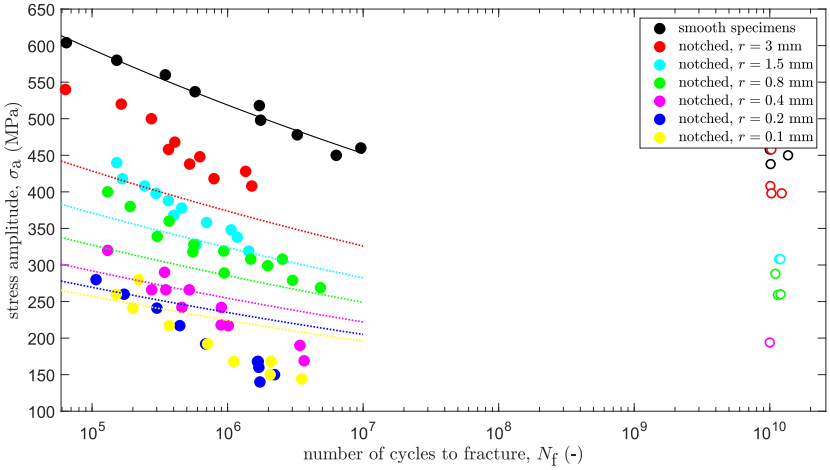

(a) $l_p = l_m(N_f = 10^7 \text{ cycles})$

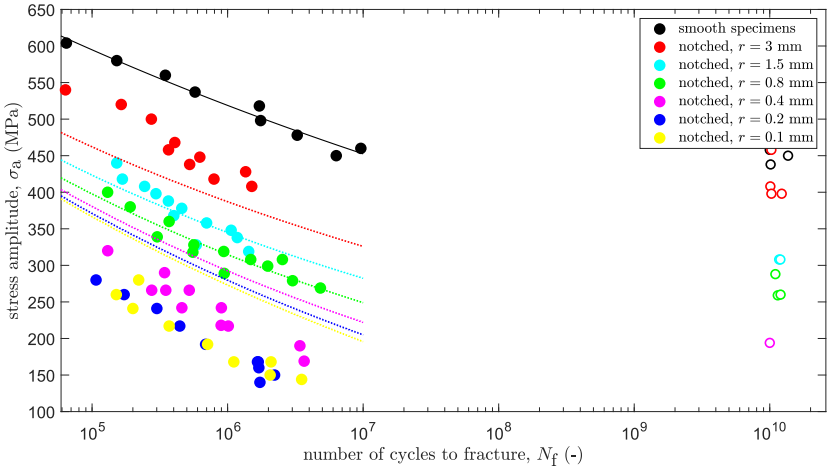

(b) $l_p(N_f) = l_m(N_f)$

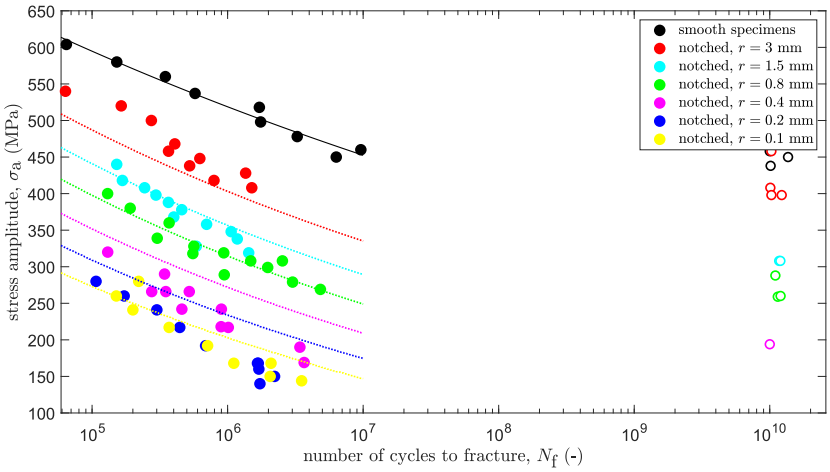

(c) $l_p(N_f) = l_m(N_f) \cdot \frac{K_{t,m}}{K_{t,p}}$

Fig. 4.8: Fatigue lifetime predictions: S690QL, model notch $r = 0.8$ mm

Conclusion

Based on the primary concept of the Theory of Critical Distances (TCD), the approach was formulated to calculate the critical distance from experimental data and numerical analyses. Sets of smooth and notched specimens with notch radii ($r = 0.1,\ 0.2,\ 0.4,\ 0.8,\ 1.5,\ 3$ mm) were tested. The critical distance was calculated for each pair of smooth and notched curves. The results show that the critical distance decreases with an increasing number of cycles to failure. This decrease is not negligible. Furthermore, it was confirmed that the critical distance significantly depends on the size of the notch and on the level of the stress concentration of the notch, making it impossible to use a single critical distance value for different geometries without modification. It was shown that the sharper the notch, the smaller the critical distance.

A total of six materials were tested: aluminium alloy AW7075, two stainless steels 1.4306 and 1.4307, and structural steels S460NL, S690QL, and S960QL. From the comparison of the average critical distances, a relationship between the critical distance and the yield strength R_p was found. As R_p increases, the average critical distance of the material decreases. The critical distance ranged from 0 to 2.5 mm, with the maximum value of 2.5 mm corresponding to half the diameter of the tested specimens. On average, the highest critical distance among the tested materials was found in stainless steel, with an average critical distance of 0.85 mm at 10^7 cycles. The lowest critical distances, zero values, were calculated for the S960QL structural steel.

The critical distance calculated using a model notch, specifically a notch with a radius of 0.8 mm, was used for fatigue life predictions. Using this critical distance, the life predictions were calculated and compared with the experimental data. Three types of calculations were performed, differing in the critical distance used for the notch life predictions:

- Constant value of critical distance, $l_\mathrm{p} = l_\mathrm{m}(N_\mathrm{f} = 10^7\mathrm{cycles})$;
- Critical distance depending on the number of cycles to fracture, $l_\mathrm{p}(N_\mathrm{f}) = l_\mathrm{m}(N_\mathrm{f})$;
- Critical distance modified by ratio of stress concentration factors, $l_\mathrm{p}(N_\mathrm{f}) = l_\mathrm{m}(N_\mathrm{f}) \cdot \frac{K_\mathrm{t,m}}{K_\mathrm{t,p}}$.

When using a constant value of critical distance, the predictions are, in most cases, unsatisfactory, mainly due to the inappropriate slope of the predicted curves. When the critical distance is made dependent on the number of cycles to fracture, the predicted curves show better alignment in slope with the experimental data. However, this approach leads to overly conservative predictions for notches with radii of $r = 1.5$ and 3 mm, while predictions for sharper notches ($r = 0.1,\ 0.2,\ 0.4$ mm) tend

to be non-conservative. In short, the spacing between the predicted curves is not ideal. This issue can be resolved by modifying the critical length parameter using the ratio of the stress concentration factor of the model notch to the stress concentration factor of the predicted notch. The proposed modification adjusts the spacing between the prediction curves for the various notched specimens accordingly. The resulting modification used is not the best or fully consistent with the experimental data in all cases, but compared to the other two tested methods, it provides the most reliable results.

The modified method was verified using different model notches ($r = 0.1$, 0.8, and 3 mm); however, it is not possible to conclude which model notch can be generally recommended for the most accurate predictions, as it depends on the material. What is essential is that the model notch is well manufactured with very smooth surface, i.e. free of machining marks, and that the experimental data exhibit minimal scatter. In general, the more similar the size of the model notch is to that of the predicted notch, the more accurate the results are.

The surface irregularities of the notches were the main issue behind the unexpected trends in the experimental data. In the case of the aluminium alloy, visible tool marks, the so-called micro-notches, were present on the surface. These surface imperfections significantly affected the behavior of the critical distances and, consequently, the resulting predictions. All smooth specimens were perfectly polished to eliminate such influences.

As expected, in the case of notched samples, the initiation of fatigue cracks on the surface was observed. In the case of sharp notches, multiple crack initiations were observed on the surface. For blunt notches, the crack often initiated from 1 to 3 locations on the surface. The number of initiation sites increases with increasing load amplitude. Regarding the failure of smooth specimens, in any case a fish-eye fracture was not observed. Only in the case of the aluminium alloy, the fracture surface was rough, and in some cases subsurface crack initiation occurred.

The main contributions of the work can be divided into three categories.
Practical Contribution:

- Design of geometries for smooth and notched specimens suitable for ultrasonic loading at 20 kHz,
- Verification of the applicability of a constant critical distance for life prediction of notched specimens,
- Verification of the applicability of a cycle-dependent critical distance for life prediction of notched specimens,
- Proposal of a modification to the critical parameter for more accurate life predictions.

Theoretical Contribution:

- Methodology for calculating the critical distance and its application for fatigue life prediction,
- Analysis of the critical length parameter in relation to material, number of cycles to failure, and notch size.

Educational Contribution:

- Description of the ultrasonic pulsator testing apparatus and a user guide for its operation,
- Summary of general knowledge on gigacycle fatigue and the Theory of Critical Distances.

The main contribution of this work is the extension of the Theory of Critical Distances (TCD) approach into the field of high cycle and gigacycle fatigue, the proposal of a modified prediction method, and its verification using experimental data. The research was carried out on samples of the same diameter, differing only in notch radius. The actual size of the real components was not considered in this study and may represent an interesting direction for further research into TCD approaches. A significant factor influencing the value of the critical distance was the surface irregularities of the notches. Incorporating these real surface data into the prediction model - specifically modifying the critical distances accordingly - could lead to even more accurate predictions.

Bibliography

[1] Shigley, R. G. B. J. K. N. J. E. *Shigley's mechanical engineering design*. 9th edth ed. McGraw-Hill, 2011. McGraw-Hill series in mechanical engineering. ISBN 9780073529288; 0073529281.

[2] Bathias. There is no infinite fatigue life in metallic materials. *Fatigue & fracture of engineering materials & structures*. Wiley Online Library. 1999, vol. 22, no. 7, p. 559–565.

[3] Sharma, A., Oh, M. C. and Ahn, B. Recent advances in very high cycle fatigue behavior of metals and alloys—a review. *Metals*. MDPI. 2020, vol. 10, no. 9, p. 1200.

[4] Boků̊vka, O., Nicoletto, G., Guagliano, M., Kunz, L., Palček, P. et al. *Fatigue of materials at low and high frequency loading*. Zilina University Publisher, 2014.

[5] Kazymyrovych, V. Very high cycle fatigue of engineering materials: A literature review. Karlstad University. 2009.

[6] Bathias, C. Piezoelectric fatigue testing machines and devices. *International Journal of Fatigue*. Elsevier. 2006, vol. 28, no. 11, p. 1438–1445.

[7] Ilie, P., Lesperance, X. and Ince, A. Development of an ultrasonic fatigue testing system for gigacycle fatigue. *Material Design & Processing Communications*. Wiley Online Library. 2020, vol. 2, no. 6, p. e120.

[8] Ruben, P. M. *Study of the fatigue strength in the gigacycle regime of metallic alloys used in aeronautics and off-shore industries*. 2010. Dissertation. Arts et Métiers ParisTech.

[9] Bathias, C. Gigacycle fatigue of high strength steels prediction and mechanisms. In: *European Structural Integrity Society*. Elsevier, 2000, vol. 26, p. 163–171.

[10] Mughrabi, H. and Antolovich, S. D. A tribute to Claude Bathias–Highlights of his pioneering work in Gigacycle Fatigue. *International Journal of Fatigue*. Elsevier. 2016, vol. 93, p. 217–223.

[11] Bathias, C., Drouillac, L. and Le Francois, P. How and why the fatigue S–N curve does not approach a horizontal asymptote. *International journal of fatigue*. Elsevier. 2001, vol. 23, p. 143–151.

[12] Liao, D., Zhu, S.-P., Correia, J. A., De Jesus, A. M. and Berto, F. Recent advances on notch effects in metal fatigue: A review. *Fatigue & Fracture of Engineering Materials & Structures*. Wiley Online Library. 2020, vol. 43, no. 4, p. 637–659.

[13] Dowling, N. E. *Mechanical Behavior of Materials eBook: International Edition*. Pearson Higher Ed, 2013.

[14] Klesnil, M. and Lukáš, P. *Fatigue of metallic materials*. Elsevier, 1992.

[15] Gough, H. J. and Pollard, H. The strength of metals under combined alternating stresses. *Proceedings of the institution of mechanical engineers*. SAGE Publications Sage UK: London, England. 1935, vol. 131, no. 1, p. 3–103.

[16] Neuber, H. *Theory of notch stresses: Principles for exact stress calculation*. JW Edwards, 1946.

[17] Molski, K. and Glinka, G. A method of elastic-plastic stress and strain calculation at a notch root. *Materials Science and Engineering*. Elsevier. 1981, vol. 50, no. 1, p. 93–100.

[18] Krzyzak, D., Robak, G. and Łagoda, T. Equivalent fatigue zone in a notched elements determined by use of non-local line method with weight function. *Solid State Phenomena*. Trans Tech Publ. 2016, vol. 250, p. 77–84.

[19] Susmel, L. and Taylor, D. The Modified Wöhler Curve Method applied along with the Theory of Critical Distances to estimate finite life of notched components subjected to complex multiaxial loading paths. *Fatigue & Fracture of Engineering Materials & Structures*. Wiley Online Library. 2008, vol. 31, no. 12, p. 1047–1064.

[20] Susmel, L. and Taylor, D. Can the conventional high-cycle multiaxial fatigue criteria be re-interpreted in terms of the theory of critical distances? *Structural Durability & Health Monitoring*. Tech Science Press. 2006, vol. 2, no. 2, p. 91.

[21] Susmel, L. The theory of critical distances: a review of its applications in fatigue. *Engineering Fracture Mechanics*. Elsevier. 2008, vol. 75, no. 7, p. 1706–1724.

[22] Taylor, D. The theory of critical distances. *Engineering Fracture Mechanics*. Elsevier. 2008, vol. 75, no. 7, p. 1696–1705.

List of the author's publications

[I] Klusák, J., Fintová, S., Kozáková, K., Jambor, M. and Seitl, S. Risk volume effect in very high cycle fatigue of 304L stainless steel. *International Journal of Fatigue.* Elsevier. 2024, vol. 178, p. 108016.

[II] Kozáková, K., Klusák, J. and Fintová, S. The length parameter for gigacycle fatigue life predictions of notched specimens made of 304L steel. *International Journal of Fatigue. Elsevier.* 2024, vol. 178, p. 107980.

[III] Kozáková, K. and Klusák, J. Fatigue lifetime predictions of notched specimens based on the critical distance and stress concentration factors. *Theoretical and Applied Fracture Mechanics.* Elsevier. 2024, vol. 133, p. 104579.

[IV] Doubek, P., Kozáková, K., Kunz, L. and Seitl, S. Fatigue life of S960 high strength steel with laser cladded functional surface layers. *Engineering Failure Analysis.* Elsevier. 2024, vol. 164, p. 108629.

[V] Sarkar, A., Klusák, J., Kozáková, K. and Christ, H.-J. Very High Cycle Fatigue Behavior of Austenitic Stainless Steel in Annealed and Predeformed Condition. *Materials Performance and Characterization.* American Society of Mechanical Engineers Digital Collection. 2023, vol. 12, no. 2.

[VI] Kozáková, K., Trávníček, L., Poduška, J. and Klusák, J. Critical length parameter of HDPE and its use in fatigue lifetime predictions. *Fracture and Structural Integrity.* 2025, vol. 19, no. 71, p. 211–222.

[VII] Kozákova, K. and Klusák, J. Fracture Mechanics Assessment of Notches Subjected to Very High-Cycle Fatigue Loading. In: *Fatigue and Fracture of Materials and Structures: Contributions from ICMFM XX and KKMP2021.* Springer, 2022, p. 299–305.

[VIII] Kozáková, K. and Klusák, J. The Prediction of Fatigue Life of Notched Specimens. *Trans VSB TU Ostrava.* Vysoká škola báňská-Technická univerzita Ostrava. 2021, vol. 21, p. 29–35.

[IX] Kozáková, K. and Klusák, J. Determination of Critical Length Parameter for Fatigue Lifetime Predictions of Notched Specimens. *Trans VSB TU Ostrava.* Vysoká škola báňská-Technická univerzita Ostrava. 2022, vol. 22, p. 16–21.

[X] Kozáková, K., Trávníček, L., Klusák, J., Poduška, J. and Hutař, P. The Influence Of Different Notches On Fatigue Lifetime Of Round Bar Specimens Made Of HDPE. *Trans VSB TU Ostrava.* Vysoká škola báňská-Technická univerzita Ostrava. 2023, vol. 23, p. 1–4.

[XI] Klusák, J., Kozáková, K., Fintová, S. and Seitl, S. Fatigue lifetimes of 1.4306 and 1.4307 stainless steels subjected to ultrasonic loading. *Procedia Structural Integrity.* Elsevier. 2022, vol. 42, p. 1369–1375.

[XII] Kozáková, K., Fintová, S. and Klusák, J. Fatigue life of notches: an effect of manufacturing. *Procedia Structural Integrity.* Elsevier. 2022, vol. 42, p. 270–275.

[XIII] Kozáková, K. and Klusák, J. Prediction of the fatigue life of notched specimens: The influence of the surface quality produced by machining. *Procedia Structural Integrity.* Elsevier. 2023, vol. 43, p. 178–183.

[XIV] Klusák, J., Kozáková, K., Jambor, M. and Seitl, S. Fatigue behavior of DIN 1.4307 and DIN 1.4306 stainless steels under high frequency loading. *Procedia Structural Integrity.* Elsevier. 2023, vol. 43, p. 142–147.

[XV] Kozáková, K., Klusák, J., Fintová, S. and Seitl, S. The effect of risk volume on the fatigue life of stainless steels subjected to high-frequency loading. *Procedia Structural Integrity.* Elsevier. 2023, vol. 51, p. 145–151.